Triplet Superconducting Pairing and Density-Wave Instabilities in Organic Conductors

J. C. Nickel,[1,2] R. Duprat,[1] C. Bourbonnais,[1] and N. Dupuis[2,3]

[1]*Regroupement Québecois sur les Matériaux de Pointe, Département de Physique, Université de Sherbrooke, Sherbrooke, Québec, Canada, J1K-2R1*

[2]*Laboratoire de Physique des Solides, CNRS UMR 8502, Université Paris-Sud, 91405 Orsay, France*

[3]*Department of Mathematics, Imperial College, 180 Queen's Gate, London SW7 2AZ, United Kingdom*

(Received 25 February 2005; published 5 December 2005)

Using a renormalization group approach, we determine the phase diagram of an extended quasi-one-dimensional electron gas model that includes interchain hopping, nesting deviations, and both intrachain and interchain repulsive interactions. We find a close proximity of spin-density- and charge-density-wave phases and singlet d-wave and triplet f-wave superconducting phases. There is a striking correspondence between our results and recent puzzling experimental findings in the Bechgaard salts, including the coexistence of spin-density-wave and charge-density-wave phases and the possibility of a triplet pairing in the superconducting phase.

DOI: 10.1103/PhysRevLett.95.247001 PACS numbers: 74.70.Kn, 71.10.Li, 74.20.Mn

Since the discovery of organic superconductivity made in the Bechgaard $(TMTSF)_2X$ salts more than two decades ago [1], the difficulty of determining the origin of this phase remains one of the main focal points of the physics of low dimensional conductors. The experimental weight given recently to the hypothesis in favor of a triplet rather than singlet superconducting phase in these compounds [2–5] raises the problem of the microscopic conditions that can lead to triplet pairing in correlated quasi-one-dimensional (quasi-1D) metals. This problem takes on particular importance in the Bechgaard salts series for which superconductivity in the phase diagram turns out to be surrounded by dominant spin-density-wave (SDW) correlations as one moves along the pressure, the temperature, or the magnetic field scale [6–8]. Repulsive intrachain interactions, which are at the root of SDW correlations, are well known to promote unconventional singlet pairing for superconductivity, whenever nesting properties of the quasi-1D Fermi surface deteriorate under pressure [9]. In the framework of the quasi-1D electron gas model with repulsive intrachain interactions, the application of the renormalization group (RG) method, which allows one to go beyond mean-field and RPA-like theories, has shown that, for sufficiently large nesting deviations, the interchain electron pairing mediated by antiferromagnetic fluctuations becomes invariably singular in the singlet interchain "d-wave" channel [10,11].

On the other hand, the extent to which weaker but present charge fluctuations can act in expanding the range of pairing possibilities is much less understood. For repulsive intrachain interactions, it was found from RPA-like approaches that charge-density-wave (CDW) fluctuations enhance pairing correlations in the triplet "f-wave" channel [12], a result that agrees with the Kohn-Luttinger mechanism for high–odd–angular momentum pairing induced by Friedel oscillations in isotropic systems [13]. Recent RG calculations showed, however, that, for repulsive intrachain interactions in the quasi-1D case, the interchain f-wave correlations always remain subordinate to those of the d-wave channel [11].

Given that charges interact through the Coulomb interaction, not only intrachain but also interchain interactions for electrons are present in practice. The key role of interchain Coulomb interaction in the stabilization of a CDW ordered state in most Peierls quasi-1D organic conductors has been made abundantly clear in the past [14–16]. Their physical relevance in the Bechgaard salts has been borne out by the puzzling observation of a CDW state that actually coexists with SDW [17,18]. In this Letter, we give the first RG determination of the phase diagram for an extended quasi-1D electron gas model that includes interchain hopping, nesting deviations, and both intrachain and interchain repulsive interactions. The last interactions turn out to have a sizable impact on the structure of the phase diagram. Unexpectedly, we find that, for a reasonably small amplitude of interchain interaction, the d-wave superconducting (SC) ordered state is destabilized to the benefit of a triplet f-wave phase with a similar range of T_c. The latter phase is preceded by dominant antiferromagnetic correlations in the normal phase and by SDW order at small nesting deviations. In these conditions, the SDW state is found to be quite close in stability to a CDW phase.

We consider weakly coupled conducting chains with a quasi-1D electron dispersion $\epsilon(k_\parallel, k_\perp) - \mu = v_F(|k_\parallel| - k_F) - 2t_\perp \cos k_\perp - 2t'_\perp \cos 2k_\perp$, where v_F is the longitudinal Fermi velocity. The interchain hopping amplitude $t_\perp$ is small with respect to the longitudinal bandwidth $2\Lambda_0$, so that the Fermi surface consists of two warped quasi-1D sheets around $k_\parallel = \pm k_F$. The next-nearest-neighbor hopping in the transverse direction, $t'_\perp \ll t_\perp$, is used to parametrize deviations from perfect nesting, which tend to suppress the SDW instability. We do not consider the small interchain hopping in the third direction, which does not play an important role in our calculation, although its

existence is crucial for the stabilization of true long-range order at finite temperature. Within the framework of an extended g-ology model, we write the bare interaction amplitude as ($j = 1, 2, 3$)

$$g_j(k'_{\perp 1}, k'_{\perp 2}, k_{\perp 2}, k_{\perp 1}) = g_j + 2g_j^{\perp} \cos(k'_{\perp 1} - k_{\perp 1}), \quad (1)$$

where $k_{\perp 1}\sigma, k_{\perp 2}\sigma'$ ($k'_{\perp 1}\sigma, k'_{\perp 2}\sigma'$) are the transverse momenta and spins of the two incoming (outgoing) particles. g_1 and g_2 correspond to backward and forward scattering, respectively, and g_3 to longitudinal umklapp processes with a lattice momentum transfer $\mathbf{G} = (4k_F, 0)$. The transverse momentum dependence comes from the nearest-neighbor interchain interactions. Longer range (bare) interactions in the transverse direction are expected to be very weak and are ignored. In this Letter, we consider only the physically relevant case of repulsive interactions ($g_j, g_j^{\perp} > 0$). For the intrachain interaction constants, we take $\tilde{g}_1 = 0.32$, $\tilde{g}_2 = 0.64$, and $\tilde{g}_3 = 0.02$, which fall into a realistic range of values compatible with various experiments in the Bechgaard salts [7,9,19–21]. The small (half-filling) umklapp process amplitude $\tilde{g}_3$ comes from the slight dimerization along the organic chains [19]. $\tilde{g}_j = g_j/\pi v_F$ and $\tilde{g}_j^{\perp} = g_j^{\perp}/\pi v_F$ are dimensionless interaction constants. The bandwidth is taken to be $2\Lambda_0 = 30t_{\perp}$, with $t_{\perp} = 200$ K. Since the values of the interchain interaction amplitudes $\tilde{g}_i^{\perp}$ are poorly known, we take them as free parameters with the only constraint that they remain smaller than the intrachain interaction amplitudes [22]. The latter condition is fulfilled in most CDW systems [15,16]. In order to minimize the number of independent parameters, we restrict the discussion to the cases $\tilde{g}_1^{\perp} = \tilde{g}_2^{\perp}$ and $\tilde{g}_3^{\perp}/\tilde{g}_3 = \tilde{g}_1^{\perp}/\tilde{g}_1$; this turns out to be sufficient to understand the global picture that emerges from our results. These show no qualitative change over a sizable range of intrachain interaction parameters. The key experimental control parameters are temperature and pressure. Pressure affects $t_{\perp}$, $\tilde{g}_j, \tilde{g}_j^{\perp}$, and $t'_{\perp}$. However, its main effect is to increase $t'_{\perp}$ and, therefore, deteriorate the nesting property of the Fermi surface.

There are different ways to implement the RG approach to a quasi-1D system [10,23]. We use the so-called one-particle irreducible momentum-shell scheme as developed in Ref. [23]. One-loop RG equations for the two-particle vertices and susceptibilities are solved numerically by dividing the Fermi surface into 2×32 patches. We retain only the $k_{\perp}$ dependence of the (running) couplings $g_j(k'_{\perp 1}, k'_{\perp 2}, k_{\perp 2}, k_{\perp 1})$. Various instabilities of the normal phase are signaled by the divergence of the corresponding susceptibilities.

For $\tilde{g}_i^{\perp} = 0$, the phase diagram has already been discussed in Ref. [10]. When the nesting of the Fermi surface is nearly perfect (small $t'_{\perp}$), the ground state is a SDW. Above a threshold value of $t'_{\perp}$, the low-temperature SDW instability is suppressed and the ground state becomes a $d_{x^2-y^2}$-wave superconducting (SCd) state with an order parameter $\Delta_r(k_{\perp}) \propto \cos k_{\perp}$ [$r = +/-$ denotes the right/left sheet of the quasi-1D Fermi surface].

The $T = 0$ phase diagram in the presence of interchain interactions ($\tilde{g}_j^{\perp} > 0$) is shown in Fig. 1. For weak interchain interactions, we reproduce the phase diagram obtained in Ref. [10]. As the interchain interactions increase, the region of stability of the d-wave SC phase shrinks, and a triplet f-wave (SCf) phase [$\Delta_r(k_{\perp}) \propto r \cos k_{\perp}$)] appears next to the d-wave phase for $\tilde{g}_1^{\perp} \simeq 0.1$. The sequence of phase transitions as a function of $t'_{\perp}$ then becomes SDW $\rightarrow$ SCd $\rightarrow$ SCf. For larger values of the interchain interactions, the SCd phase disappears and the region of stability of the f-wave SC phase widens. In addition, a CDW phase appears, thus giving the sequence of phase transitions SDW $\rightarrow$ CDW $\rightarrow$ SCf as a function of $t'_{\perp}$. For $\tilde{g}_1^{\perp} \gtrsim 0.12$, the SDW phase disappears. Note that, for $\tilde{g}_1^{\perp} \simeq 0.11$, the region of stability of the CDW phase is very narrow, and there is essentially a direct transition between the SDW and SCf phases.

The transition temperature of the SDW phase is not very sensitive to the values of the interchain interactions. The transition temperature of the SC phase decreases for $\tilde{g}_1^{\perp} \lesssim 0.1$ (i.e., when the SC phase shrinks in the $T = 0$ phase diagram) and increases for $\tilde{g}_1^{\perp} \gtrsim 0.1$ (i.e., when the $T = 0$ SC phase widens). Our RG calculations yield $T_c \sim 30$ K for the SDW phase in the case of perfect nesting and $T_c \sim 0.6$–1.2 K for the SC phase, in fair agreement with experiments in the Bechgaard salts. Figure 2 shows the transition temperature T_c as a function of $t'_{\perp}$ for three different values of the interchain interactions, $\tilde{g}_1^{\perp} = 0$, 0.11, and 0.14, corresponding to the three different sequences of phase transitions as a function of $t'_{\perp}$: SDW $\rightarrow$ SCd, SDW $\rightarrow$ (CDW) $\rightarrow$ SCf, and CDW $\rightarrow$ SCf.

In the absence of interchain interactions, the effective interaction mediated by spin fluctuations is attractive in the $d_{x^2-y^2}$- and f-wave channels. It is repulsive in the p_x- [$\Delta_r(k_{\perp}) \propto r$] (at variance with a phenomenological approach to superconductivity [24]), the p_y- ($\sin k_y$), and d_{xy}-wave ($r \sin k_{\perp}$) channels. The d-wave correlations

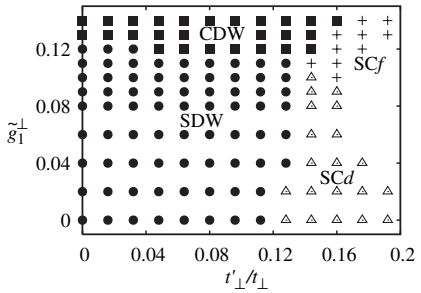

FIG. 1. $T = 0$ phase diagram as a function of $t'_{\perp}/t_{\perp}$ and $\tilde{g}_1^{\perp} = \tilde{g}_2^{\perp}$ (with $\tilde{g}_3^{\perp}/\tilde{g}_3 = \tilde{g}_1^{\perp}/\tilde{g}_1$). Circles: SDW; squares: CDW; triangles: SCd [$\Delta_r(k_{\perp}) \propto \cos k_{\perp}$]; crosses: SC$f$ [$\Delta_r(k_{\perp}) \propto r \cos k_{\perp}$].

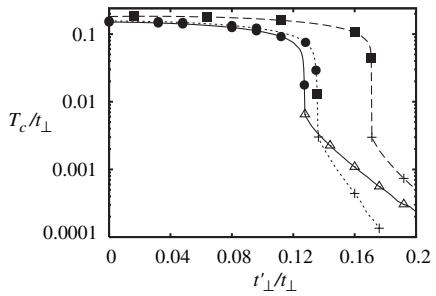

FIG. 2. Transition temperature as a function of $t'_\perp/t_\perp$ for $\tilde{g}_1^\perp = 0$, 0.11, and 0.14, corresponding to the solid, dotted, and dashed lines, respectively.

dominate over the f-wave ones, as they involve the three components of the spin fluctuations. The origin of the f-wave SC and CDW phases can be understood by considering the contribution of the $g_j^\perp$'s to the (bare) scattering amplitudes in the singlet and triplet particle-particle channels, as well as in the charge and spin channels. $g_1^\perp$ favors $(2k_F, \pi)$ CDW and triplet SC fluctuations but suppresses the singlet SC fluctuations; it does not affect SDW fluctuations. There is also an indirect effect, since CDW fluctuations, via the usual mechanism of fluctuation exchange, enhance triplet SC fluctuations and suppress singlet SC fluctuations. A similar analysis shows that $g_2^\perp$ has a detrimental effect on both singlet and triplet nearest-neighbor chain SC pairing. Nevertheless, the RG calculation shows that weak intrachain umklapp processes (as present in the Bechgaard salts) are sufficient to neutralize this effect through an enhancement of both spin and charge fluctuations. As for the interchain umklapp processes ($g_3^\perp$), they oppose the effect of g_3, thus pushing the occurrence of the CDW and SCf phases to slightly higher values of $\tilde{g}_1^\perp = \tilde{g}_2^\perp$.

The RG approach also provides important information about the fluctuations in the normal phase. It has already been pointed out that the dominant fluctuations above the SCd phase are SDW fluctuations [10], as observed experimentally [7]. Although the SDW fluctuations saturate below $T \sim t'_\perp$, where the SCd fluctuations increase, the latter dominate only in a very narrow temperature range above the SC transition (Fig. 3). Above the SCf and CDW phases, one expects strong CDW fluctuations driven by $g_1^\perp$. Figures 4 and 5 show that, for $\tilde{g}_1^\perp \sim 0.11$–$0.12$, strong SDW and CDW fluctuations coexist above the SCf phase. Remarkably, there are regions of the phase diagram where the SDW fluctuations remain the dominant ones in the normal phase above the SCf or CDW phase (Fig. 5).

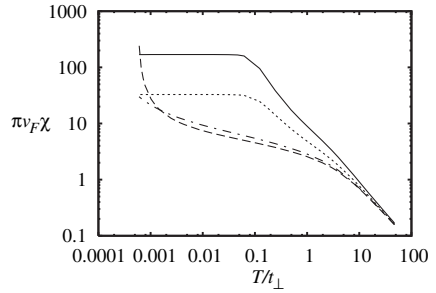

FIG. 3. Temperature dependence of the susceptibilities in the normal phase above the SCd phase [$t'_\perp = 0.152t_\perp$ and $\tilde{g}_1^\perp = 0.08$]. The solid line corresponds to SDW, the dotted line to CDW, the dashed line to SCd, and the dashed-dotted line to SCf correlations, which already show enhancement.

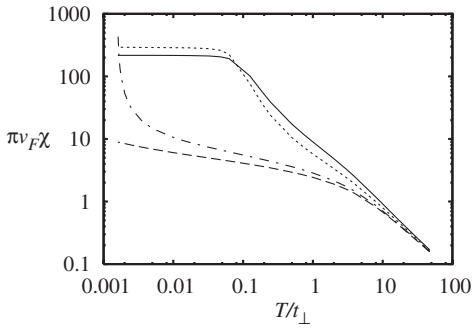

FIG. 4. Temperature dependence of the susceptibilities in the normal phase above the SCf phase [$t'_\perp = 0.152t_\perp$ and $\tilde{g}_1^\perp = 0.12$].

A central result of this Letter is the close proximity of SDW, CDW, and SCf phases in the phase diagram of a quasi-1D conductor with a *realistic* range of values for the repulsive interactions. Although this proximity is found only in a small range of interchain interactions, there are several features of our results that suggest that this part of the phase diagram is the relevant one for the Bechgaard salts. (i) SDW fluctuations remain important in the normal phase throughout the whole phase diagram; they dominate above the SCd phase and remain strong (sometimes even being dominant) above the SCf phase where they coexist with strong CDW fluctuations, in accordance with observations [7,18]. (ii) The SCf and CDW phases stand nearby in the theoretical phase diagram; the CDW phase is always closely following the SCf phase when the interchain interactions increase. This agrees with the experimental find-

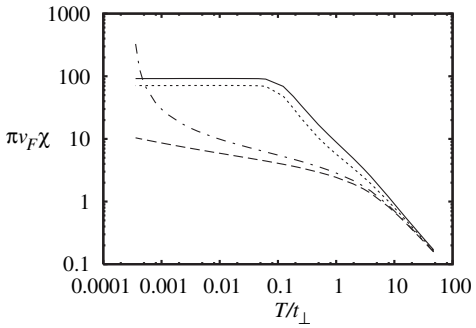

FIG. 5. Same as Fig. 4 but for $t'_\perp = 0.176t_\perp$.

ing that both SDW and CDW coexist in the DW phase of the Bechgaard salts [17] and the existence, besides SDW correlations, of CDW fluctuations in the normal state above the SC phase [18]. (iii) Depending how one moves in practice in the phase diagram as a function of pressure in Fig. 1, our results are compatible with either a singlet d-wave or a triplet f-wave SC phase in the Bechgaard salts. Moreover, we cannot exclude that both SCd and SCf phases exist in these materials, with the sequence SDW $\rightarrow$ SCd $\rightarrow$ SCf under pressure. It is also possible that the SCf phase, not sensitive to the Pauli pair breaking effect, is stabilized by a magnetic field [11,25]. This would provide an explanation for the existence of large upper critical fields exceeding the Pauli limit [3,4] and for the temperature independence of the NMR Knight shift in the SC phase [5]. Finally, the predicted existence of nodes in the SC gap for the d- and f-wave scenarios may appear in contradiction with the thermal conductivity and specific heat jump measurements for the Bechgaard salt $(TMTSF)_2ClO_4$, which are apparently consistent with a nodeless order parameter [26]. Owing to the anion lattice superstructure of this compound, however, an ''anion'' gap $\Delta_X \gg T_c$ must be taken into account in the calculations so that a direct comparison with the RG method can be made.

J. C. N. is grateful to the Gottlieb Daimler- und Karl Benz-Stiftung for partial support. C. B. thanks D. Jérome, Y. Fuseya, M. Tsuchiizu, Y. Suzumura, L. G. Caron, and S. Brown for useful discussions.

[1] D. Jérome, A. Mazaud, M. Ribault, and K. Bechgaard, J. Phys. (Paris), Lett. **41**, L95 (1980).
[2] L. P. Gor'kov and D. Jérome, J. Phys. (Paris), Lett. **46**, L643 (1985).
[3] I. J. Lee, M. J. Naughton, G. M. Danner, and P. M. Chaikin, Phys. Rev. Lett. **78**, 3555 (1997).
[4] J. I. Oh and M. J. Naughton, Phys. Rev. Lett. **92**, 067001 (2004).
[5] I. J. Lee, S. E. Brown, W. G. Clark, M. J. Strouse, M. J. Naughton, W. Kang, and P. M. Chaikin, Phys. Rev. Lett. **88**, 017004 (2002).
[6] D. Jérome and H. Schulz, Adv. Phys. **31**, 299 (1982).
[7] P. Wzietek, F. Creuzet, C. Bourbonnais, D. Jérome, K. Bechgaard, and P. Batail, J. Phys. I (France) **3**, 171 (1993).
[8] P. Chaikin, J. Phys. I (France) **6**, 1875 (1996).
[9] V. J. Emery, Synth. Met. **13**, 21 (1986); M. T. Béal-Monod, C. Bourbonnais, and V. J. Emery, Phys. Rev. B **34**, 7716 (1986); L. G. Caron and C. Bourbonnais, Physica (Amsterdam) **143B+C**, 453 (1986).
[10] R. Duprat and C. Bourbonnais, Eur. Phys. J. B **21**, 219 (2001).
[11] Yuki Fuseya and Yoshikazu Suzumura, J. Phys. Soc. Jpn. **74**, 1263 (2005).
[12] K. Kuroki, R. Arita, and H. Aoki, Phys. Rev. B **63**, 094509 (2001); Y. Tanaka and K. Kuroki, Phys. Rev. B **70**, 060502(R) (2004); S. Onari, R. Arita, K. Kuroki, and H. Aoki, Phys. Rev. B **70**, 094523 (2004).
[13] W. Kohn and J. M. Luttinger, Phys. Rev. Lett. **15**, 524 (1965).
[14] L. P. Gor'kov and I. E. Dzyaloshinskii, Zh. Eksp. Teor. Fiz. **67**, 397 (1974) [Sov. Phys. JETP **40**, 198 (1974)]; P. A. Lee, T. M. Rice, and R. A. Klemm, Phys. Rev. B **15**, 2984 (1977).
[15] S. Barišić and A. Bjeliš, in *Theoretical Aspects of Band Structures and Electronic Properties of Pseudo-One-Dimensional Solids*, edited by H. Kaminura (Reidel, Dordrecht, 1985), p. 49.
[16] J. P. Pouget and R. Comes, in *Charge Density Waves in Solids*, edited by L. P. Gor'kov and G. Gruner (Elsevier Science, Amsterdam, 1989), p. 85.
[17] J. P. Pouget and S. Ravy, J. Phys. I (France) **6**, 1501 (1996); S. Kagoshima, Y. Saso, M. Maesato, R. Kondo, and T. Hasegawa, Solid State Commun. **110**, 479 (1999).
[18] N. Cao, T. Timusk, and K. Bechgaard, J. Phys. I (France) **6**, 1719 (1996).
[19] V. J. Emery, R. Bruinsma, and S. Barišić, Phys. Rev. Lett. **48**, 1039 (1982).
[20] A. Schwartz, M. Dressel, G. Grüner, V. Vescoli, L. Degiorgi, and T. Giamarchi, Phys. Rev. B **58**, 1261 (1998).
[21] C. Bourbonnais and D. Jérome, in *Advances in Synthetic Metals, Twenty Years of Progress in Science and Technology*, edited by P. Bernier, S. Lefrant, and G. Bidan (Elsevier, New York, 1999), pp. 206–261.
[22] K. Šaub, S. Barišić, and J. Friedel, Phys. Lett. **56A**, 302 (1976).
[23] C. Honerkamp, M. Salmhofer, N. Furukawa, and T. M. Rice, Phys. Rev. B **63**, 035109 (2001); B. Binz, D. Baeriswyl, and B. Douçot, Ann. Phys. (N.Y.) **12**, 704 (2003).
[24] A. G. Lebed, K. Machida, and M. Osaki, Phys. Rev. B **62**, R795 (2000).
[25] H. Shimahara, J. Phys. Soc. Jpn. **69**, 1966 (2000).
[26] S. Belin and K. Behnia, Phys. Rev. Lett. **79**, 2125 (1997); P. Garoche R. Brusetti, D. Jérome, and K. Bechgaard, J. Phys. (Paris), Lett. **43**, L147 (1982). It should be emphasized that, for the $(TMTSF)_2ClO_4$ compound, the nodes of the d-wave and f-wave order parameters, which occur at $k_\perp = \pm\pi/2$, are precisely located where a gap opens due to the ClO_4 ordering at 24 K $\gg$ T_c(SC), thus making these two phases effectively nodeless. For a more detailed discussion of the BCS d-wave case, see H. Shimahara, Phys. Rev. B **61**, R14 936 (2000).